JOURNAL OF MATERIALS SCIENCE **40** (2005) 3939–3943

Studies of Fe-doped SiO_2/TiO_2 composite nanoparticles prepared by sol-gel-hydrothermal method

ZHIJIE LI, BO HOU
State Key Laboratory of Coal Conversion, Institute of Coal Chemistry, Chinese Academy of Sciences, Taiyuan, 030001, People's Republic of China; Graduate School of Chinese Academy of Sciences, Beijing 100039, People's Republic of China

YAO XU, DONG WU, YUHAN SUN*
State Key Laboratory of Coal Conversion, Institute of Coal Chemistry, Chinese Academy of Sciences, Taiyuan, 030001, People's Republic of China

Fe-doped SiO_2/TiO_2 composite nanoparticles were directly prepared by sol-gel-hydrothermal process, and characterized by X-ray diffraction (XRD), transmission electron microscope (TEM), thermal gravimetry (TG), X-Ray photoelectron spectroscopy (XPS), and UV-Vis diffuse reflectance spectra (DRS). It was found that the Fe^{3+} was well dispersed in solid solution of SiO_2/TiO_2 composite nanoparticles that was about 10 nm with spherical morphology and rich silica layer external surface. It could effectively offer broadband shield for both UVB (290–320 nm) and UVA (320–400 nm). The results of Photodecomposition of methylene blue showed that the photoactivity of Fe-doped SiO_2/TiO_2 composite was minimized due to the addition of iron ion.
© *2005 Springer Science + Business Media, Inc.*

1. Introduction

It is well known that titania (TiO_2) nanoparticles can effectively offer broadband shield for both parts of the terrestrial UV radiation, the short wavelength UV range (UVB: 290–320 nm) and the longer wavelength range (UVA: 320–400 nm) [1, 2]. As anti-UV reagent, titania is chemically inert, non-toxic and non-irritating, so it was widely used cosmetics, paint, plastics, and so on [3, 4]. However, because of strong oxidation potentials of the electron-depleted valence band on the surface of photoexcited TiO_2 nanoparticles, it may accelerate photodegradation reaction of some organic ingredients in these products [5, 6]. Additionally, good dispersibility of TiO_2 is very advantageous in enhancing their UV screening efficiency. But TiO_2 nanoparticles are easy to agglomerate and their shield effectivity reduced drastically. So, it is necessary to decrease the photoactivity of TiO_2 nanoparticles and enhance its dispersibility.

It was reported that coated TiO_2 particles with oxide or hydroxide compounds of aluminum, silicon, iron, zirconium, cerium and phosphorus could minimize the photoactivity of TiO_2 nanoparticles and prevent aggregation [7–9]. However, it was complex to deposit hydroxide or oxide on the surfaces of fine titania nanoparticles, and the coating process leads to insufficient shielding effect to ultraviolet radiation in the range of UVA.

In the current work, Fe-doped SiO_2/TiO_2 composite nanoparticles with good dispersibility and low photoactivity were directly prepared by sol-gel-hydrothermal method. The primary properties and effective factors were discussed and the photoactivity was examined.

2. Experimental

2.1. Synthesis of samples

0.202 g of $Fe(NO_3)_3 \cdot 9H_2O$ was added to 55 ml of 2 $mol \cdot L^{-1}$ nitric acid solution. At 50°C, 11.2 ml of tetraethylorthosilicate (TEOS) was added with magnetic stirring and a sol was formed. Then 17.0 ml of titanium *n*-butoxide (TB) was added dropwise to the above solution under magnetic. After stirred for 20 min, a gel was formed and was transferred into a Teflon-lined autoclave to hydrothermal react at 140°C for 10 h. Finally; the resulted product was dried at 120°C to obtain the sample 1.0%Fe-SiO_2/TiO_2 composite nanoparticles, in which 1.0% refers to the weight percentage of Fe in samples. Different samples of 2.0%Fe-SiO_2/TiO_2 and 3.0%Fe-SiO_2/TiO_2 were also prepared through the same method by varying the content of added $Fe(NO_3)_3 \cdot 9H_2O$.

2.2. Characterization of samples

The crystalline phase of particles were determined using X-ray diffraction (XRD) performed on a D/max

*Author to whom all correspondence should be addressed.

2500 diffractometer, (40 kV, 30 mA, Cu K_α radiation). The morphology of particles was observed by transmission electron microscope (TEM, Hitachi-600-2). The BET surface area was calculated by nitrogen adsorption at 77 K on Tristar 3000 (Micromeritics, Co.). The thermal gravimetry (TG) analysis was carried out on Perkin-Elmer TGA-2 thermal gravimeter in air from room temperature to 1000°C at a heating rate of 10°C/min. The element composition and the chemical state of particle surface were determined by X-Ray photoelectron spectroscopy (XPS, PHI5300X, Perkin-Elmer Physics Electronics, Mg K_α as radiation source). UV-Vis diffuse reflectance spectra (DRS) were measured on Shimadzu UV-2101 apparatus, equipped with an integrating sphere, using $BaSO_4$ as reference.

2.3. Photodecomposition of methylene blue (MB)

The photochemical reactor was consisted of a cylindrical jacketed quartz tube with 5.0 cm in diameter and 27 cm in length. A 300 W highly pressure mercury vapor lamp with a wavelength at 365 nm was placed inside the reactor. The light source assembly was placed concentrically inside the 300 ml Pyrex glass container of 6.0 cm in diameter and 28.5 cm height filled with 250 ml MB solution. The distance between the source and bottom of the vessel was 1.5 cm to aid for better stirring using a magnetic stirrer. To keep the temperature of the solution during the reaction, water was circulated through the annulus of the jacket quartz tube. The MB concentration was 100 ppm with a catalyst loading of 0.5 kg/m^3. Before irradiation, the suspension aqueous solution was stirred continuously in dark for 30 min to ensure adsorption/desorption equilibrium. The adsorption equilibrium concentration was used as the initial value for the further kinetic treatment of the photodecomposition processes. Samples were collected from the mixture solution at regular intervals and centrifuged to analyze by Shimadzu UV-2101 apparatus to determine the concentration of MB.

3. Results and discussion

3.1. The crystalline phase of particles

The XRD patterns of Fe-doped SiO_2/TiO_2 composite nanoparticles were shown in Fig. 1. All samples were anatase phase before and after calcined at 400°C. In addition, no characteristic peaks of iron oxides phases appeared, this suggested that iron distribution was possibly continuous in the particles. The crystalline grain size of TiO_2 in samples calculated by Scherrer formula decreased from 8.5 to 6.5 nm when the Fe^{3+} content increased from 0.0 to 3.0%. After calcined at 400°C, the crystalline grain sizes of TiO_2 in SiO_2/TiO_2 composite nanoparticles increased to 10.3 nm and in 3%Fe-doped composite nanoparticles were 8.5 nm. At the same time, Fig. 1 suggested a decrease of crystallinity in the Fe-doped SiO_2/TiO_2 composite nanoparticles in comparison with the undoped sample, indicated by the decrease in the intensity of TiO_2 peaks, it suggested that the addition of Fe^{3+} could occupy regular lattice site of TiO_2 and might distort crystal structure of the host compound.

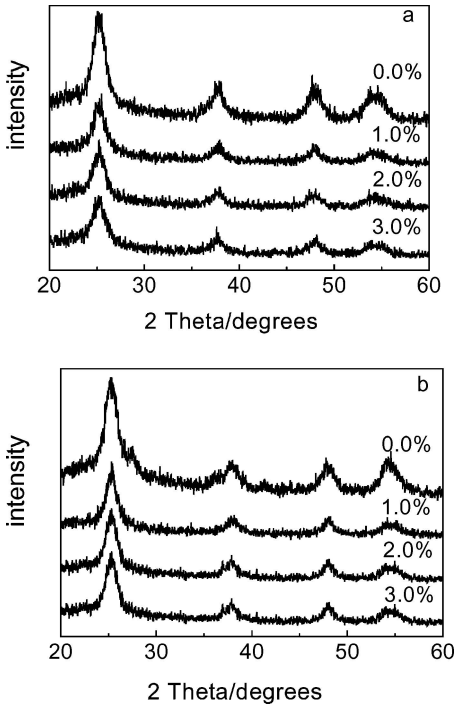

Figure 1 XRD patterns of Fe-doped SiO_2/TiO_2 composite nanoparticles with different Fe content (a) Before calcined, (b) Calcined at 400°C for 2 h.

3.2. The morphologies of nanoparticles

The TEM images of SiO_2/TiO_2 and 3.0%Fe-SiO_2/TiO_2 composite nanoparticles are shown in Figs 2 and 3. The SiO_2/TiO_2 nanoparticles was well dispersed and spherical with narrow size distribution before and after calcined at 400°C. The particles slightly aggregated and grew from 10 nm to 14 nm after calcined at 400°C. The 3% Fe-SiO_2/TiO_2 composite nanoparticles with the size of 10 nm were more dispersed and uniformed than that of SiO_2/TiO_2 even calcined at 400°C. Both narrow size distribution nanoparticles and excellent dispersibility were in favor of anti-UV reagent.

The BET special surface area of SiO_2/TiO_2 and 3%Fe-SiO_2/TiO_2 composite nanoparticles were increased from 181.6 to 254.7 $m^2 \cdot g^{-1}$ and 304 to 394.6 $m^2 \cdot g^{-1}$ after calcined at 400°C for 2 h, respectively. During the calcination process, the remaining organic byproduct after hydrothermal reaction and the adsorbed water were removed, so the BET special surface area was increased.

3.3. TG analysis

The weight loss curves of samples were drawn in Fig. 4. The weight loss of SiO_2/TiO_2 and 3%Fe-SiO_2/TiO_2 composite nanoparticles were 4.84 and 7.42% before 250°C, respectively, which were the desorption of adsorbed water and expulsion of adsorbed organic fraction. The weight loss of them was 9.27 and 11.30% from 250 to 490°C, respectively, which could contribute to dehydroxylation and decomposition of the organic fraction. This also implied that some organics

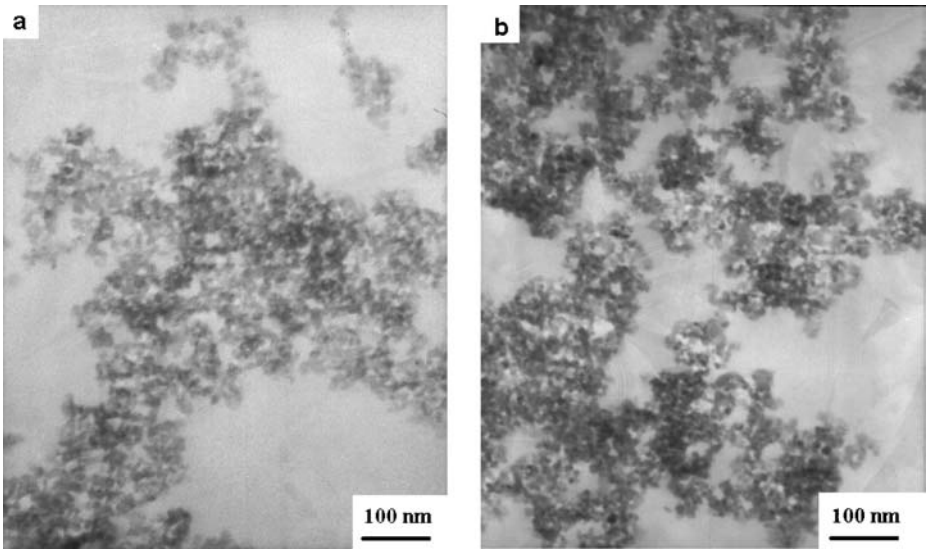

Figure 2 TEM images of SiO_2/TiO_2 composite nanoparticles (a) Before calcinations, (b) Calcined at 400°C for 2 h.

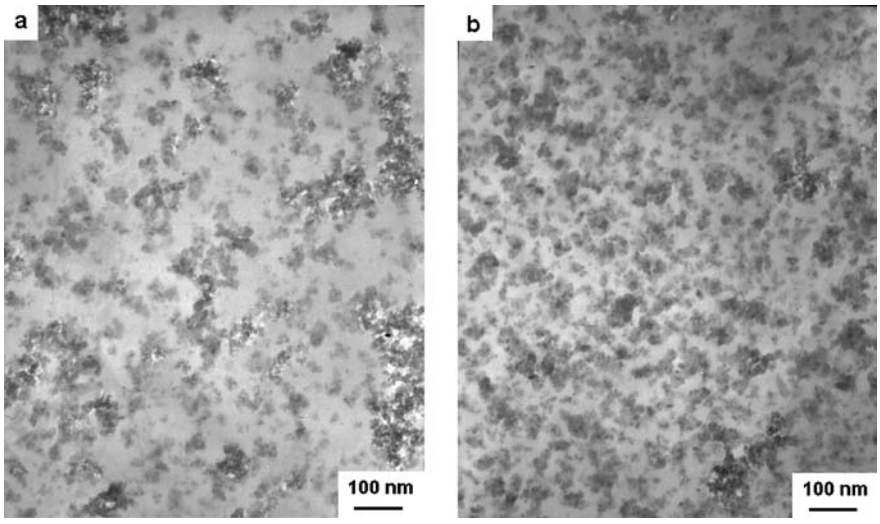

Figure 3 TEM images 3.0%Fe-SiO_2/TiO_2 composite nanoparticles (a) Before calcined, (b) Calcined at 400°C for 2 h.

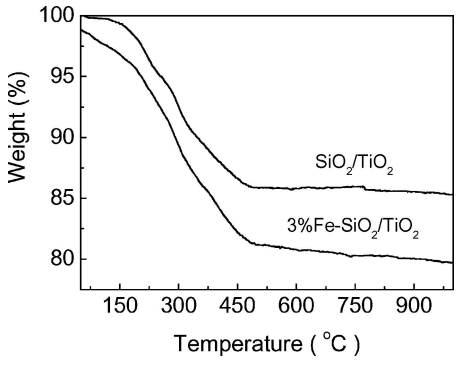

Figure 4 TG curves of SiO_2/TiO_2 and 3%Fe-SiO_2/TiO_2 composite nanoparticles.

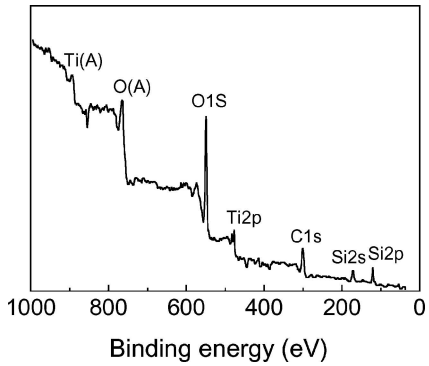

Figure 5 The XPS spectra of 3.0%Fe-SiO_2/TiO_2 composite nanoparticles.

byproduct incorporated into samples during hydrothermal process.

3.4. XPS analysis

XPS spectrum of 3%Fe-SiO_2/TiO_2 is shown in Fig. 5. It was found that there was no iron on the surface because the Fe2p characteristic peaks around 711 eV did not appeared [12]. It indicated that iron inserted into the matrix interior of SiO_2/TiO_2 composite nanoparticles. The ionic radius of Ti^{4+} is 0.068 nm, and the Fe^{3+} is 0.064 nm, so the Fe^{3+} ions could substitute Ti^{4+} to form stable solid solutions. The less amounts of iron than the nominal ones calculated from these XPS data had been reported in the Fe-doped titania prepared by sol-gel method [10]. On the other hand, the surface atomic percentages of Si and Ti were 79.0 and 21.0 calculated

from XPS data, did not correspond to the original percentages (50.0%) in the mixtures, respectively. So an external surface silica rich layer was formed in the sol-gel-hydrothemal procedure.

3.5. UV-Vis diffuse reflectance spectra (DRS)

The diffuse reflectance spectra of samples with different Fe content were depicted in Fig. 6. The spectra of Fe-doped SiO_2/TiO_2 composite nanoparticles displayed a red shift in the band gap transition with the dopant content. It was reported that the shift resulted from the incorporation of Fe ions into the TiO_2 nanoparticles [11, 12]. Red shifts of this type could be attributed to the charge-transfer transitions between the iron ion *d* electrons and the TiO_2 conduction or valence band. The Fe-doped SiO_2/TiO_2 composite nanoparticles showed excellent absorption in the longer wavelength range (UVA: 320–400 nm) than that of SiO_2/TiO_2 composite nanoparticles, which was favorable for anti-UV reagent. On the other hand, there was no separated phase of iron oxide because its broad band centered at 500 nm was not appeared [13]. This was another evidence that the iron doped with SiO_2/TiO_2 nanoparticles rather than existed as iron oxide.

In the visible range, the Fe-doped SiO_2/TiO_2 composite nanoparticles after caclined at 400°C showed higher absorptions than the undoped SiO_2/TiO_2 composite nanoparticles, and this absorption increased with the iron content, together with changes on color from pale yellow to brown. Same changes in color had been reported in the case of Fe-doped TiO_2 specimens compared with pure TiO_2 [10, 13, 14]. All uncaclined as-prepared SiO_2/TiO_2 and Fe-SiO_2/TiO_2 series particles were brown, so they showed higher absorptions in the visible range than that after calcined.

3.6. Photodecomposition of methylene blue (MB)

The photocatalytic decomposition kinetics of MB on samples was given in Fig. 7. The Fe-SiO_2/TiO_2 composite nanoparticles had lower photocatalytic activity than that of SiO_2/TiO_2 composite nanoparticles. Before reaction, approximately 42–52% of MB was adsorbed by the uncalcined samples; while 20–30% MB was adsorbed by the calcined samples. In Fig. 7a, the SiO_2/TiO_2 composite nanoparticles had higher photocatalytic activity and the concentration of MB could be decreased to 5 ppm in 65 min. However, the Fe-SiO_2/TiO_2 composite nanoparticles had lower photocatalytic activity and the concentration of MB was changed very less. Because of the remove of the organic byproduct after calcined at 400°C, the photocatalytic activity of samples increased. However, the Fe-SiO_2/TiO_2 still exhibited lower photocatalytic activity than SiO_2/TiO_2 composite nanoparticles.

The special surface areas, particle size and the crystallinity must be considered in comparison the photocatalytic activity among these samples. Because all samples were in anatase phase, the variation in photocatalytic activity could not originate from the difference of crystal phase. The larger surface area and smaller particle average size of the Fe-SiO_2/TiO_2 composite nanoparticles should be in favor of high photocatalytic activity, but this was inconsistent with experimental

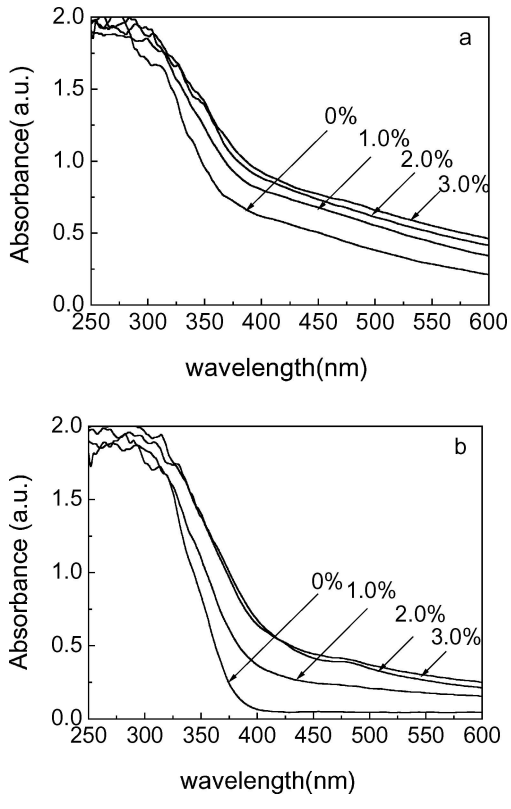

Figure 6 The diffuse reflectance spectra of samples with different Fe contents (a) Before calcined, (b) Calcined at 400°C for 2 h.

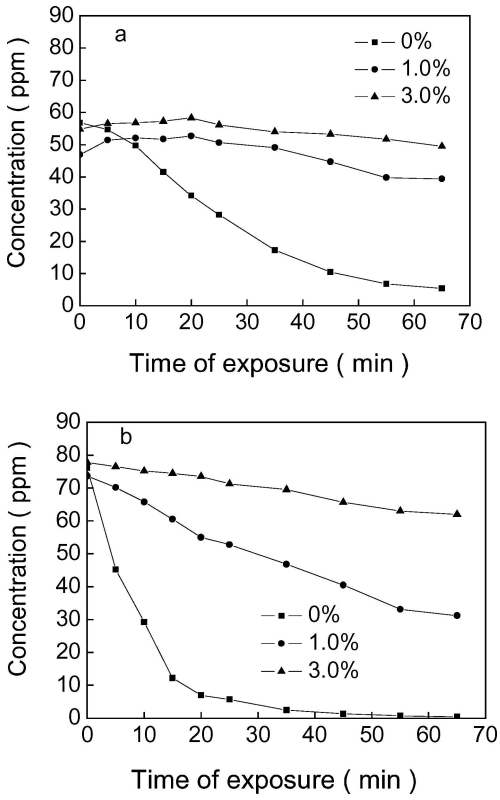

Figure 7 Kinetics of the photocatalytic decomposition of MB on samples with different Fe contents (a) before calcination, (b) calcined at 400°C for 2 h.

results. So the addition of iron should only be responsible for the resulted low photocatalytic activity.

It is generally assumed that a higher photoactivity for Fe-doped titania is possible in comparison with the undoped material, principally because of enhanced lifetimes of electrons and holes [11, 12, 15]. However, as Fe^{3+} inserted into the matrix interior of SiO_2/TiO_2 composite nanoparticle, the role of the iron ions was different. Doped Fe^{3+} was isolated far from the surface with a much lower chance of transferring trapped charge carriers to the interface. As a result, the Fe^{3+} were more likely to serve as recombination centers than as trap sites for eventual charge transfer at the interface. Thus, Fe-doped SiO_2/TiO_2 composite nanoparticles show decreased photoreactivities.

4. Conclusions

In summary, a spherical Fe-doped SiO_2/TiO_2 composite nanoparticles about 10 nm with well dispersibility were directly prepared by sol-gel-hydrothermal method. It could effectively offer broadband shield for both parts of the terrestrial UV radiation. XPS analysis showed that a well-dispersed dilute solid solution of Fe^{3+} in SiO_2/TiO_2 composite nanoparticles with external surface silica rich layer. The Fe^{3+} was inserted into the matrix interior. As a result, the photoactivity of Fe-doped SiO_2/TiO_2 was lowered. So the Fe-doped SiO_2/TiO_2 composite nanoparticles prepared by sol-gel-hydrothermal method is a promising anti-UV reagent to be used in cosmetics, paint, plastics, and the like.

Acknowledgement

The work is supported by National Native Science Foundation of China (Grant No. 20133040).

References

1. J. SCHULZ, H. HOHENBERG, F. PFUCKER, E. GARTNER, T. WILL, S. PFEIFFER, R. WEPF, V. WENDEL, H. G. BARLAG and K. P. WITTERN, *Adv. Drug Delivery Rev.* **54** (2002) S157.
2. R. G. MOLEN, H. M. H. HURKS, C. O. LUITING, F. SPIES, J. NOORDENDE, H. K. KOERTEN and A. M. MOMMAAS, *J. Photochem. Photobio. B* **44** (1998) 143.
3. M. HOFFMANN, S. MARTIN, W. CHOI and D. BAHNENANN, *Chem. Rev.* **95** (1995) 69.
4. T. THERSTON and J. WILCOXON, *J. Phys. Chem. B* **103** (1999) 11.
5. C. THIERRY, D. DOMINIQUE and P. BERNARD, US6,187,438 (2001).
6. G. WIEDERHOFT, K. BUTJE, P. J. BARENTHIEN, M. BODIGER and H. ALBERTS, US5,840,111 (1998).
7. G. DRANSFIELD, P. J. GUEST, P. L. LYTH, D. J. MCGARVEY and T. G. TRUSCOTT, *J. Photochem. Phtobio. B* **59** (2000) 147.
8. S. V. MANORAMA, K. M. REDDY, C. V. G. REDDY, S. NARAYANAN, P. R. RAJA and P. R. CHATTERJI, *J. Phys. Chem. Solids.* **63** (2002) 135.
9. L. ZIOLKOWSKI, K. VINODGOPAL and P. V. KAMAT, *Langmuir* **13** (1997) 3124.
10. J. A. NAVIO, G. COLON, M. MACIAS, C. REAL and M. I. LITTER, *Appl. Catal. A: General* **177** (1999) 111.
11. W. CHOI, A. TERMIN and M. R. HOFFMANN, *J. Phys. Chem.* **98** (1994) 13669.
12. C. WANG, D. W. BAHNEMANN and J. K. DOHRMANN, *Chem. Commun.* (2000) 1539.
13. J. A. NAVIO, G. COLON, M. I. LITTER and G. N. BIANCO, *J. Mol. Catal.* **106** (1996) 267.
14. M. I. LITTER and J. A. NAVIO, *J. Photochem. Photobiol. A* **84** (1994) 183.
15. J. SORIA, J. C. CONESA, V. AUGUGLIARO, L. PALMISANO, M. SCHIAVELLO and A. SCLAFANI, *J. Phys. Chem.* **95** (1991) 274.

Received 22 November 2004
and accepted 15 February 2005